

An effective Approach for Damage Detection using Reduction Model Technique and Optimization Algorithms

Long Nguyen Ngoc^a , Thanh Bui-Tien^a , Hoa Tran-Ngoc^{a*} 

^aDepartment of Bridge Engineering & Underground Infrastructure, Faculty of Civil Engineering, University of Transport and Communications, Hanoi, Vietnam. Email: nguyennngoclong@utc.edu.vn, btthanh@utc.edu.vn, ngochoa@utc.edu.vn

* Corresponding author

<https://doi.org/10.1590/1679-78257696>

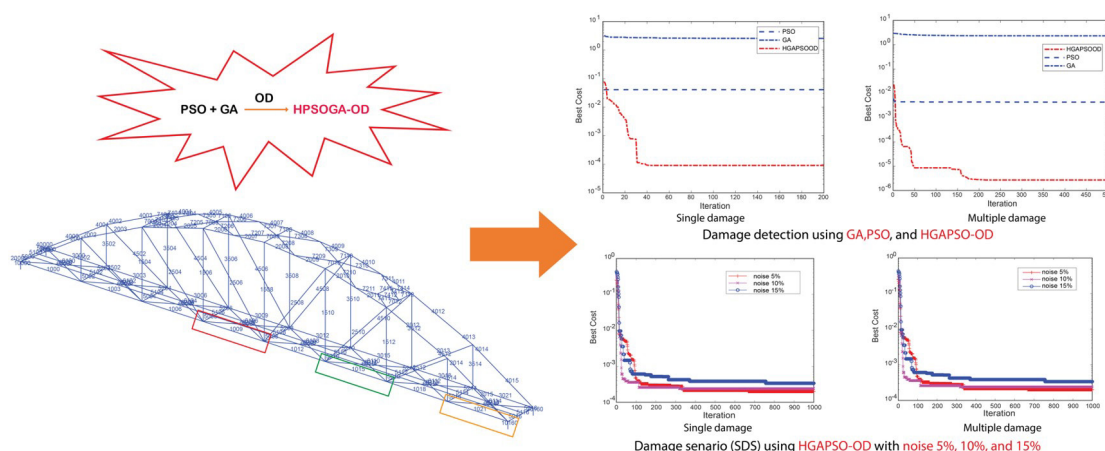
Abstract

With the development of science and technology in recent decades, numerous optimization algorithms have emerged and been successfully applied in various fields. Particle swarm optimization (PSO) is a well-established evolutionary algorithm commonly used for optimization tasks. However, similar to other evolutionary algorithms, PSO has two main limitations that can hinder its performance. The first limitation is premature convergence, which can result in suboptimal solutions. The second limitation is the high computational time since PSO employs all particles in the swarm for each iteration. To overcome these limitations, in this work, we propose coupling a reduction model technique, specifically, Orthogonal Diagonalization (OD) with a hybrid algorithm combining Genetic Algorithm (GA) and PSO, termed HGAPSO-OD. To evaluate the effectiveness of the proposed approach, a large-scale railway bridge, calibrated based on field measurements, is used as a case study. The results demonstrate that HGAPSO-OD not only increases the accuracy but also reduces computational time of GA and traditional PSO.

Keywords

Structural Health Monitoring, Genetic Algorithm, Particle Swarm Optimization.

Graphical Abstract



Received: April 26, 2023; In revised form: May 2, 2023; Accepted: September 11, 2023; Available online: September 15, 2023.

<https://doi.org/10.1590/1679-78257696>



Latin American Journal of Solids and Structures. ISSN 1679-7825. Copyright © 2023. This is an Open Access article distributed under the terms of the [Creative Commons Attribution License](https://creativecommons.org/licenses/by/4.0/), which permits unrestricted use, distribution, and reproduction in any medium, provided the original work is properly cited.

1 INTRODUCTION

Structural Health Monitoring (SHM) is an interdisciplinary field that has gained significant attention in recent years due to its inherent potential to safeguard the safety, reliability, and sustainability of civil infrastructure, aerospace structures, mechanical systems, and so on (Jahangiri et al., 2016; YiFei et al., 2023). SHM entails the continuous monitoring of structures through the synergistic utilization of sensing, data analysis, and decision-making techniques to comprehensively assess their condition, proactively detect any damage, and accurately predict their remaining useful life. The timely and precise information provided by SHM regarding structural integrity and performance empowers proactive maintenance and management strategies, thereby engendering heightened safety measures, diminished maintenance costs, and optimized operational efficiency (L. Ho Viet et al, 2022; Nguyen-Ngoc et al., 2023).

Over the past few decades, SHM has witnessed significant advancements in various aspects, including data acquisition, sensor technologies, predictive modeling, and decision-making algorithms (Khatir et al., 2022; Tran-Ngoc et al., 2023; Việt, Hoàng Việt, H et al., 2023). These advancements have served as a catalyst for the emergence and adoption of diverse SHM approaches and methodologies, spanning from conventional methods like visual inspection and manual monitoring to cutting-edge techniques that leverage advanced sensors, wireless communication, and machine learning algorithms. These advancements have not only widened the scope and applicability of SHM but have also presented novel prospects and complexities for researchers and practitioners in the field (Mostafa and Tawfik, 2016; Nguyen et al., 2021; Ngoc Long Nguyen et al, 2023; Tran-Ngoc et al., 2020a).

As a flexible optimization tool that operates autonomously without relying on gradient information and possesses ease of use, the metaheuristic algorithm has found diverse applications in various scenarios, as evidenced by extensive research efforts in recent years (Gholipour et al., 2013; Shahriari et al., 2016). This has led to the development of multiple high-performance algorithms that have been extensively utilized for Structural Health Monitoring (SHM), including PSO (Kennedy and Eberhart, 1995), Cuckoo Search (Yang and Deb, 2014), Differential Evolution (DE) (Das and Suganthan, 2010), Grey Wolf Optimizer (GWO) (Mirjalili et al., 2014), Dynamic Invasive Weed Optimization (DIWO) (Kenane et al., 2021), Enhanced Sine Cosine Algorithm (ESCA) (Chen et al., 2020), Moth Flame Optimization (MFO) (Mirjalili, 2015), Salp Swarm Algorithm (SSA) (Mirjalili et al., 2017), and so on.

Although PSO has been commonly applied for many fields, this algorithm still suffers from notable limitations, as it heavily relies on the efficacy of the initial particle populations. Since initial particles generate suboptimal results, it may result in the inability to identify the optimal solution, leading to failure in achieving the desired outcome. Another constraint of PSO lies in the significant computational time required, as the algorithm utilizes all particles in the swarm for each iteration, resulting in high computational cost.

To deal with the shortcomings and increase the effectiveness of traditional PSO, in this paper, an efficient hybrid approach, denoted as HGAPSO, which combines GA with mutation and crossover capabilities, along with PSO, is used to effectively address optimization challenges. Additionally, we employ OD technique to rearrange the particle positions and selectively update only the particles with the most promising solutions for subsequent iterations, resulting in a significant reduction in computational cost. HGAPSO-OD exhibits several distinctive features, including the application of HGAPSO increase the effectiveness of PSO, the use of a single guide for updating particle velocities instead of both local best and global best, and the updating of only the velocity and position of the best particles in each iteration.

To evaluate the efficacy of the HGAPSO-OD, a railway bridge exhibiting both single and multiple damages is utilized as a case study. Furthermore, careful consideration is given to the impact of various factors, including the effect of noise.

2 METHODOLOGY

PSO is highly dependent on the quality of the initial populations, as the positions of the initial particles play a crucial role in determining the success of the optimization process. When the initial particle positions are distant from the global best solution, it can pose challenges in identifying the most optimal solution. To mitigate this limitation of PSO, a hybrid approach has been proposed by integrating PSO with GA (Tran-Ngoc et al., 2020a), where in GA is employed to generate improved next generations of particles after each iteration, aiming to enhance the optimization performance. In this research paper, OD is also employed to arrange the optimal local positions of particles in the form of a matrix, and only those particles that own superior solutions (located on the diagonal line of the OD matrix) are selected for subsequent iterations. The population of particles (denoted as " n ") is divided into two distinct groups: the active group consists of b elements, and the passive group consists of $(n-b)$ elements. This division is based on the optimal solutions of elements after each iteration. The active group consists of the particles that yield better solutions, while the passive group includes the results of the remaining particles (Tran-Ngoc et al., 2020b).

The algorithm employed in this study is based on the premise that only the active group is updated during subsequent iterations, while the passive group remains unchanged due to their insignificant contributions to the search for the optimal solution. This approach effectively reduces the model's dimensionality and computational time. In each iteration, particles from the active group are used to construct a matrix (referred to as “ B ”), followed by the determination of an OD matrix (denoted as “ F ”). The objective function (referred to as “ $\varnothing(U)$ ”) is then applied to reduce the discrepancies between the calculated and actual results. The overall process of searching for the optimal solution using the combined approach of OD and GAPSO is outlined as follows:

Step 1: In the first step, the parameters of particles such as their initial position (U^0) and velocity (V^0) are given as

$$U^0 = [u_1^0, u_2^0, \dots, u_n^0]; \tag{1}$$

$$V^0 = [v_1^0, v_2^0, \dots, v_n^0]; \tag{2}$$

n indicates the population of particles.

Step 2: The optimal local solutions within the populations are determined by evaluating the objective function $\varnothing(U)$ and subsequently arranged in ascending order can be presented as

$$\varnothing(U) = \sum_{y=1}^{n_{mode}} \frac{(\tilde{f}_y - f_y)^2}{(\tilde{f}_y)^2} \tag{3}$$

$$U^0 = [U_{max}^0, \dots, U_{min}^0] \tag{4}$$

f_y and \tilde{f}_y introduce calculated and measured natural frequencies. n_{mode} , and y denote the number of modes, and the modal order, respectively.

Step 3: The best parents are chosen for crossover and mutation processes and used for the next iteration, which can be obtained as

$$G_{global_best} = [U_{max}^0] \tag{5}$$

Step 4: Repeat the process from step 2 to step 3 until termination criteria is satisfied.

Step 5: Creating a matrix T_1 that is comprised of the optimal solutions of particles, where each row represents the optimal solution of an individual particle, derived from the outcomes obtained in **step 4**. The matrix T_1 can be written as

$$T_1 = [U^j]_{(n \times m)} \tag{6}$$

m are the number of uncertain parameters.

Step 6: A square matrix B with the size $b \times b$ is developed by using the matrix T_1 , can be presented as

$$\text{For } q_1 = 1 : b; q_2 = 2 : b$$

$$B(1, q_1) = T_1(1, q_1) \tag{7}$$

$$B(q_1, 1) = T_1(1, q_1) \tag{8}$$

$$B(q_2, q_1) = T_1(q_2, q_1) \tag{9}$$

End

For $q_1 = 2 : b$

$$B_1(q_2, q_1) = B(1, q_1) \quad (10)$$

$$B(q_1, q_2) = B_1(q_2, q_1) \quad (11)$$

End

Step 7: Orthogonal diagonalization matrix F is given as

$$F = M^{-1} * B * M \quad (12)$$

Matrix M and matrix F consist of eigenvectors and the eigenvalues of matrix B , respectively.

Step 8: The search areas of particles can be written as

$$U_{lower} = [U_{min}]_{(n * m)} \quad (13)$$

$$U_{upper} = [U_{max}]_{(n * m)} \quad (14)$$

Step 9: The velocity and position of particles are updated as

$$V^{(j+1)}(i) = \mu * V^j(i) + \alpha_1 * rand * (U_{best}^{j+1}(i) - U^j(i)) + \alpha_2 * rand * (W_{best}(i) - U^j(i)) \quad (15)$$

$$U^{(j+1)}(i) = (U^j(i) + V^{(j+1)}(i)); \quad (16)$$

$$\text{If } (U^{(j+1)}(i)) > U_{upper} \quad (17)$$

$$U^{(j+1)}(i) = U_{lower} + rand * U_{lower} \quad (18)$$

$$\text{If } (U^{(j+1)}(i)) < U_{lower} \quad (19)$$

$$U^{(j+1)}(i) = U_{lower} + rand * U_{lower} \quad (20)$$

The variables α_1 and α_2 are indicative of the factors associated with cognition learning and social learning, respectively, while the term 'rand' signifies random numbers that fall within the range of 0 to 1. Additionally, the parameter μ denotes the inertia weight, while $W_{best}(i)$ and $U_{best}^{j+1}(i)$ refer to the global best and local best of element i , respectively. j and $j+1$ represent the iterations at time j and $j+1$. U_{lower} , and U_{upper} are lower and upper bounds of search areas of particles.

Step 10: The local best solution for each element is chosen, and the subsequent global best solution is determined based on the evaluation of the objective function $\varphi(U)$, which can be presented as

$$\text{If } (\varphi(U^{(j+1)}) < \varphi(U^{(j)})) \quad (21)$$

$$\varphi(U_{best}^{j+1}) = \varphi(U^{(j+1)}); U_{best}^{j+1} = U^{(j+1)} \quad (22)$$

$$\text{Otherwise } \varphi(U_{best}^{j+1}) = \varphi(U^{(j)}); U_{best}^{j+1} = U^{(j)} \quad (23)$$

Step 11. Repeating the process steps 5-10 until termination criteria are satisfied.

Step 12: The iteration is completed, and the best solution can be calculated as

$$\varnothing(W_{best}) = \min \varnothing(U^{(k)}) \tag{24}$$

$$W_{best} = U^{(k)} \tag{25}$$

k indicates k^{th} iteration; $k \in [0, N^t]$; N^t is the number of iterations.

3 DESCRIPTIONS OF THE BRIDGE

The Nam O bridge, located in the central region of Vietnam, serves as a critical link for railway traffic between the North and South regions. It has been in operation since 1950 and has been subjected to constant heavy train loads with high frequency. Over time, the bridge has experienced degradation due to defects in certain truss members, leading to reduced stiffness. Despite these issues, the bridge is still capable of carrying out its intended function under the designed loads. The bridge is comprised of four spans, each of which has a nearly equal length of 75m. Truss members are connected to each other by truss joints, and these truss joints are linked by bolts. The spans are supported by U-shaped abutments and solid piers, which are commonly utilized in railway bridges. Roller and pin bearings are employed to provide support for the spans. The main structural elements of the bridge include upper and lower chords, vertical and diagonal chords, upper and lower wind bracings, struts, and stringers. Detailed dimensions of these truss members can be found in the reference provided by (Tran-Ngoc et al., 2018). The layout of the bridge is illustrated in **Figure 1** (Tran-Ngoc et al., 2018).



Figure 1 Nam O Bridge

4 FINITE ELEMENT MODEL (FEM)

To predict structural dynamic behavior, and compare it with that obtained from measurement, a FEM of Nam O bridge was built by using the MATLAB (see **Figure 2**).

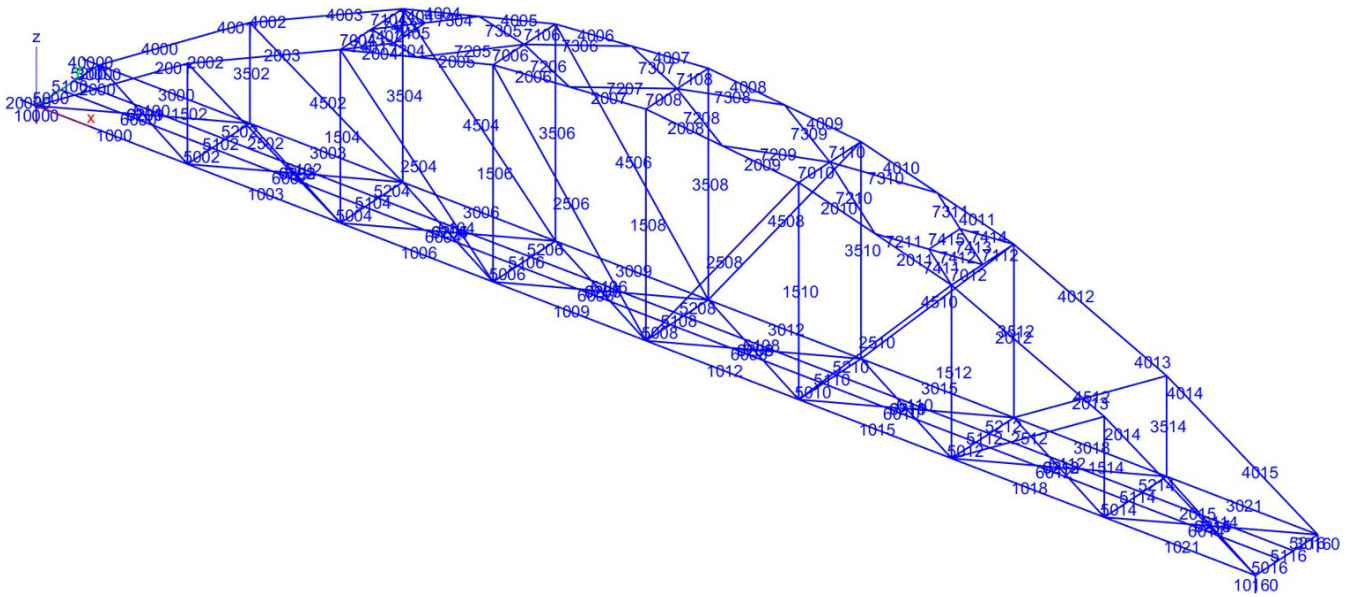


Figure 2 The FEM of Nam O Bridge.

The following specifications outline the FEM:

- The bridge is represented by 137 nodes and 227 elements, utilizing 9 different section types of truss members (Tran-Ngoc et al., 2018).
- The key structural components, such as lower chords, upper chords, diagonal chords, vertical chords, struts, lower wind bracings, upper wind bracings, and stringers are modeled using three-dimensional (3D) beam elements. These elements have six degrees of freedom at each node, encompassing translations in the x , y , and z directions, as well as rotations around the x , y , and z axes. The element incorporates the principles of Timoshenko beam theory, encompassing shear-deformation impacts. It offers choices for both unrestricted and restricted warping possibilities. Additionally, the transverse girders of the deck system are modeled using beam elements.
- The global coordinate system assigns the x -axis along the bridge's longitudinal direction, the z -axis perpendicular to the river flow direction (transverse direction), and the y -axis in the vertical direction. The left main truss corresponds to the downstream side, while the right main truss corresponds to the upstream side. These trusses depict the side view of the bridge.
- The bearings are modeled using spring elements.

From FEM, the natural frequency of the first five modes is obtained as shown in **Table 1**, which is used as objective functions to identify structural damage.

Table 1 The natural frequencies from the FEM.

Mode order	Numerical model (Hz)
1	1.45
2	3.10
3	3.27
4	4.66
5	6.55

5 DAMAGE DETECTIONS

5.1 Single damage

Three distinct locations of damage are investigated, specifically damage in proximity to the bearing (referred to as damage scenario $D1$), damage at a quarter length span (referred to as damage scenario $D2$), and damage near the center of the beam (referred to as damage scenario $D3$). These damage locations are located at elements 1009, 1015, and 1021, respectively, and have a damage rate of 50%, as illustrated in Figure 3. Damage is created by reducing the stiffness of the

elements. For example, damage rate of 50% means the stiffness of the element has decreased by 50% compared to its initial state. Subsequently, a comparative analysis of the accuracy of various algorithms, including GA, PSO, and HGAPSO-OD, is performed to assess the performance of these algorithms in detecting single damages. In the case of GA, a population size of 50 is employed and a real-coded approach is utilized with crossover and mutation operators set at 0.8 and 0.1, respectively. Regarding PSO and HGAPSO-OD, a population size of 50 is employed along with learning factors α_1 and α_2 set to 2. For both PSO and HGAPSO-OD, the inertia weight parameter (μ) is set at 0.3. The search process is considered complete when the number of iterations reaches 200 or when the fitness discrepancy between two consecutive iterations is less than 10^{-5} .

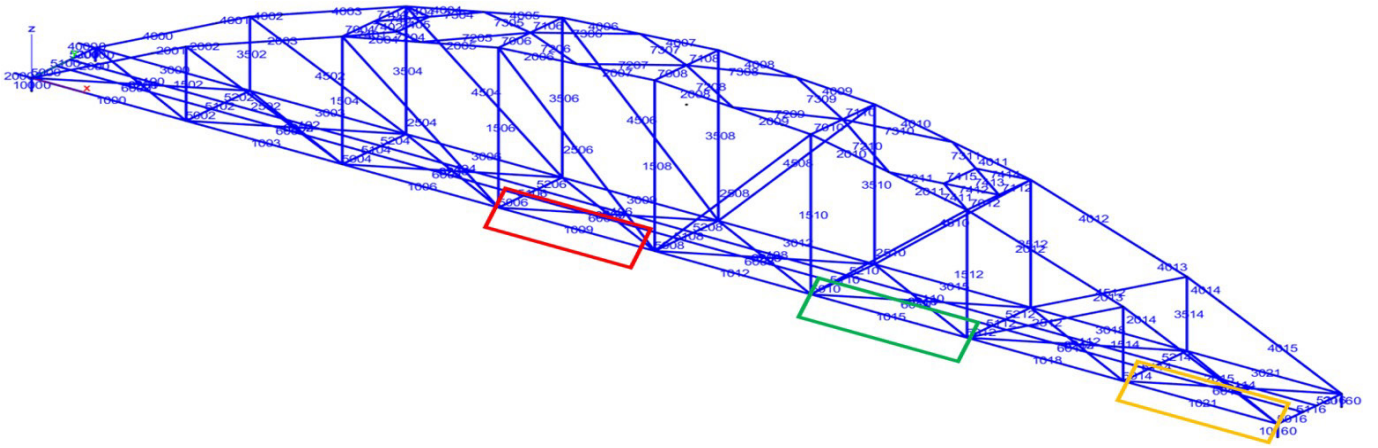


Figure 3 Single damages – damage scenario D1 to D3.

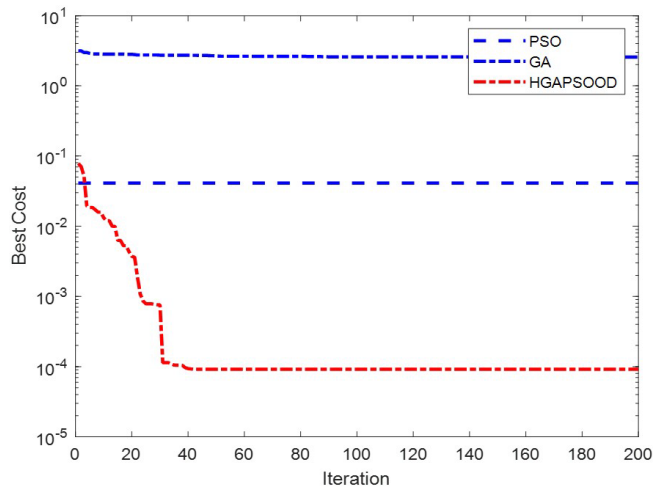


Figure 4 The accuracy of three used algorithms (D1).

Table 2 Damage detection using GA, PSO, and HGAPSO-OD for single element damage (Element 1009) – damage scenario D1.

Elements	Real damaged	GA	PSO	HGAPSO-OD
1000	0.00	0.96	0.00	0.00
1003	0.00	0.61	0.00	0.00
1009	0.60	0.83	0.00	0.60
1012	0.00	0.71	0.00	0.00
1015	0.00	0.89	0.00	0.00
1018	0.00	0.84	0.00	0.00
1021	0.00	0.82	0.00	0.00
1024	0.00	0.51	0.00	0.00
Time (second)		93.167	92.078	73.721

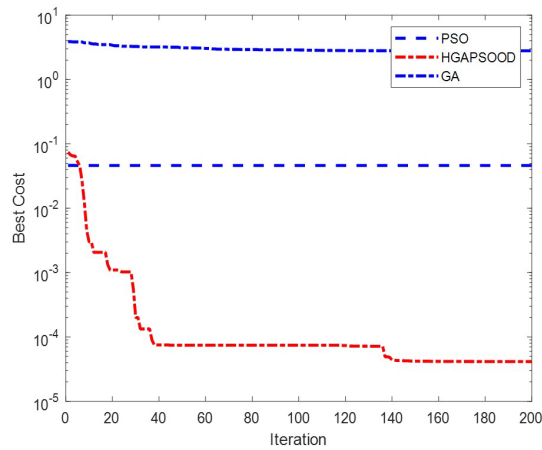


Figure 5 The accuracy of three used algorithm (D2)

Table 3 Damage detection using GA, PSO, and HGAPSO-OD for single element damage (Element 1015) – damage scenario D2.

Elements	Real damaged	GA	PSO	HGAPSO-OD
1000	0.000	0.931	0.002	0.001
1003	0.000	0.461	0.002	0.019
1006	0.000	0.914	0.002	0.001
1009	0.000	0.834	0.002	0.001
1012	0.000	0.958	0.002	0.001
1015	0.600	0.956	0.002	0.598
1018	0.000	0.945	0.002	0.002
1021	0.000	0.386	0.001	0.001
Time (second)		96.695	95.864	76.802

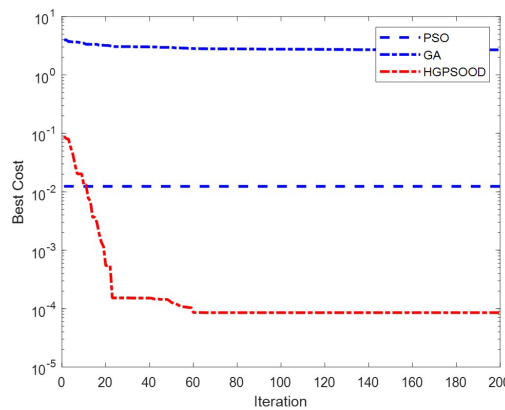


Figure 6 The accuracy of three used algorithm (D3)

Table 4 Damage detection using GA, PSO, and HGAPSO-OD for single element damage (Element 1021) – damage scenario D3.

Elements	Real damaged	GA	PSO	HGAPSO-OD
1000	0.000	0.977	0.002	0.001
1003	0.000	0.353	0.002	0.001
1006	0.000	0.935	0.002	0.001
1009	0.000	0.739	0.002	0.001
1012	0.000	0.566	0.002	0.001
1015	0.000	0.970	0.002	0.001
1018	0.000	0.761	0.002	0.001
1021	0.600	0.964	0.002	0.596
Time (second)		96.317	94.156	94.156

Through the analysis of Figure 4 to Figure 6 and Table 2 to Table 4, it becomes evident that the HGAPSO-OD method, as proposed, outperforms the GA and PSO methods in terms of accuracy. Specifically, the HGAPSO-OD method demonstrates precise prediction of actual damages in three instances, transpiring at elements 1009, 1015, and 1021, with a commendable accuracy rate of 60%. Conversely, GA and PSO exhibit erroneous identification of both the positions and severity of damage.

5.2 Multiple damages

This research investigates the occurrence of multiple damages by examining three distinct damage locations (referred to as damage scenario D4), which are positioned at elements 1009, 1015, and 1021 along the structure. The damage rates at these locations are set at 30% for element 1009, 50% for element 1015, and 10% for element 1021, as visually depicted in Figure 7.

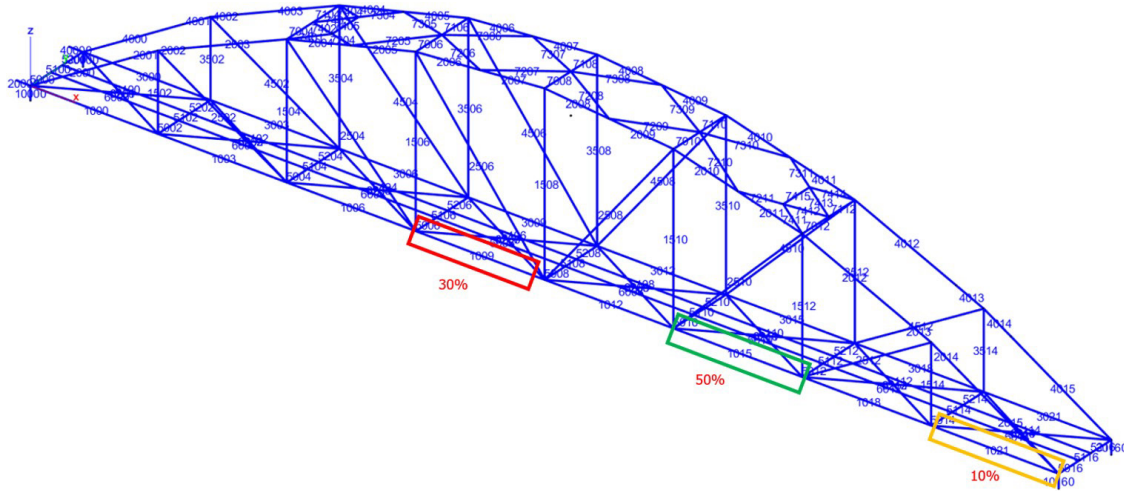


Figure 7 Multiple damage – damage scenario D4.

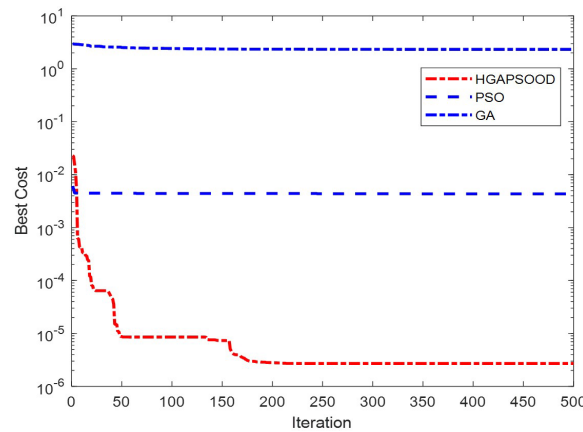


Figure 8 The accuracy of three used algorithms (D4)

Table 5 Damage detection using GA, PSO, and HGAPSO-OD for multiple damage– damage scenario D4.

Elements	Real damaged	GA	PSO	HGAPSO-OD
1000	0.000	0.998	0.001	0.001
1003	0.000	0.952	0.002	0.001
1006	0.000	0.998	0.001	0.002
1009	0.300	0.361	0.197	0.299
1012	0.000	0.994	0.001	0.001
1015	0.500	0.378	0.523	0.499
1018	0.000	0.992	0.002	0.002
1021	0.100	0.083	0.099	0.100
Time (second)		217.139	210.586	170.312

The graphical representation presented in Figure 8 elucidates that the convergence efficacy of the HGAPSO-OD method transcends that of the GA and PSO techniques. Furthermore, the findings from Table 5 provide compelling evidence that the HGAPSO-OD method exhibits a remarkable ability to precisely ascertain the locations and magnitudes of damages in the examined elements, in contrast to the struggles encountered by GA and PSO in achieving comparable accuracy in determining these critical parameters. Moreover, the utilization of the HGAPSO-OD approach consistently results in reduced computational time in comparison to both GA and PSO methods across all scenarios.

5.3 Damage detection with noise

To evaluate the influence of noise on the efficacy of the proposed method, white gaussian noise is utilized applying varying noise levels, specifically 5%, 10%, and 15%. White gaussian noise calculated by using awgn function in MATLAB can be presented as

$$f_y^n = awgn(f_y, snr) \tag{26}$$

f_y^n and f_y indicate new and old input data; snr is signal-to-noise ratio.

- Single damage

Table 6 Single Damage Scenario (SDS) with noise 5%, 10%, and 15%

Elements	Real damage	Damage with noise		
		5%	10%	15%
1000	0.000	0.001	0.001	0.001
1003	0.000	0.001	0.001	0.001
1006	0.000	0.001	0.001	0.002
1009	0.200	0.191	0.193	0.188
1012	0.000	0.003	0.001	0.001
1015	0.000	0.001	0.001	0.001
1018	0.000	0.001	0.001	0.004
1021	0.000	0.001	0.001	0.001

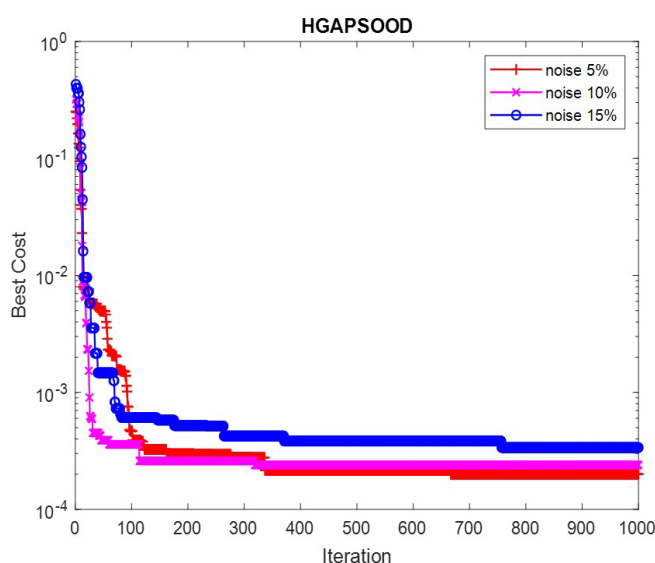


Figure 9. Single Damage Scenario (SDS) using HGAPSO-OD with noise 5%, 10%, and 15%

- •Multiple damage

Table 7 Multiple damage scenario (SDS) with noise 5%, 10%, and 15%

Elements	Real damaged	Damage with noise		
		5%	10%	15%
1000	0.000	0.001	0.025	0.002
1003	0.000	0.003	0.006	0.082
1006	0.000	0.003	0.001	0.002
1009	0.300	0.300	0.301	0.300
1012	0.000	0.001	0.039	0.051
1015	0.500	0.498	0.451	0.477
1018	0.000	0.001	0.103	0.001
1021	0.200	0.198	0.162	0.181

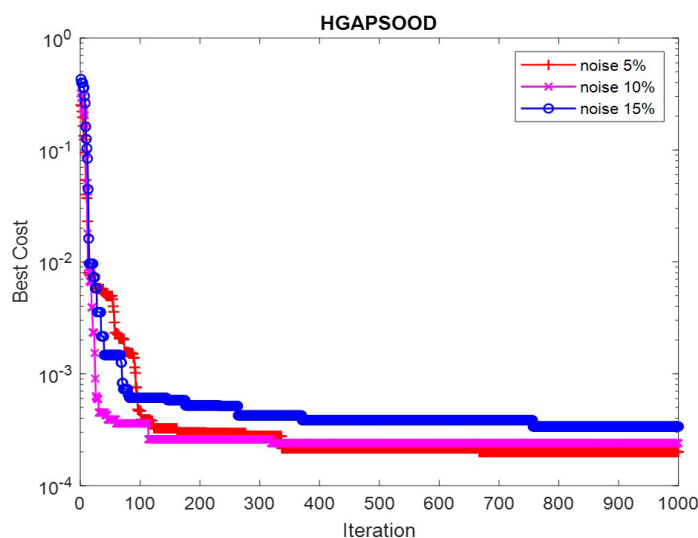


Figure 10 Multiple Damage Scenario (SDS) using HGAPSO-OD with noise 5%, 10%, and 15%

Based on the findings derived from Figure 9, Figure 10, Table 6, and Table 7, it is evident that the accuracy of the obtained results diminishes with higher levels of noise. Nevertheless, the HGAPSO-OD algorithm, as proposed, demonstrates its proficiency in accurately identifying the positions and severity of damages in the elements under consideration, even in scenarios where noise levels range from 5% to 15%, regardless of whether damages occur at 1 or 2 elements.

6. CONCLUSION

In conclusion, this paper presents an effective approach for damage detection that incorporates reduction models and optimization algorithms. The study systematically evaluates the performance of GA, PSO, and HGAPSO-OD in detecting damages in diverse scenarios. The proposed approach leverages reduction models to mitigate computational costs while maintaining accuracy and optimizes the damage detection process using the aforementioned algorithms.

The research findings demonstrate that the proposed approach achieves accurate detection of damages in various scenarios, including single damage locations and multiple damage cases. The comparative analysis of accuracy among the algorithms reveals that HGAPSO-OD outperforms GA and PSO in terms of detection accuracy. Additionally, the utilization of reduction models effectively reduces computational costs, enhancing the efficiency and practicality of the approach for real-world applications.

In order to evaluate the influence of noise on measurement outcomes, varying levels of noise (5%, 10%, and 15%) were applied within the framework of the HGAPSO-OD method. The results divulge that, despite the presence of such noise levels, the HGAPSO-OD method adeptly identifies the precise location and extent of structural damage.

The contributions of this research to the field of structural health monitoring are significant, as it presents an effective approach that integrates reduction models and optimization algorithms for damage detection. The proposed approach has the potential for practical implementation in SHM of civil infrastructure, aerospace, and mechanical systems, facilitating timely detection and mitigation of damages. However, it can be seen that the approach still has

limitations, such as low accuracy and the proposed method only being applied to simple structural numerical models. Future research should apply the proposed method to detect damage in more realistic and complex structures.

Acknowledgment

This research is funded by University of Transport and Communications (UTC) under grant number T2022-CT- 010TĐ.

Author's Contributions: Conceptualization, L. Nguyen Ngoc and H. Tran-Ngoc; Methodology, L. Nguyen Ngoc and T. Bui-Tien; Writing - original draft, L. Nguyen Ngoc and T. Bui-Tien; Writing - review & editing, H. Tran-Ngoc.

Editor: Pablo Andrés Muñoz Rojas

References

- Chen, H., Wang, M., Zhao, X., 2020. A multi-strategy enhanced sine cosine algorithm for global optimization and constrained practical engineering problems. *Applied Mathematics and Computation* 369, 124872.
- Das, S., Suganthan, P.N., 2010. Differential evolution: A survey of the state-of-the-art. *IEEE transactions on evolutionary computation* 15, 4–31.
- Gholipour, Y., Shahbazi, M.M., Behnia, A., 2013. An improved version of Inverse Distance Weighting metamodel assisted Harmony Search algorithm for truss design optimization. *Latin American Journal of Solids and Structures* 10, 283–300.
- Hoàng Việt, H., Đỗ Anh, T., Phạm Đức, T., 2023. Utilizing artificial neural networks to anticipate early-age thermal parameters in concrete piers. *Transport and Communications Science Journal* 74, 445–455. <https://doi.org/10.47869/tcsj.74.4.5>
- Jahangiri, V., Mirab, H., Fathi, R., Etefagh, M.M., 2016. TLP structural health monitoring based on vibration signal of energy harvesting system. *Latin American Journal of Solids and Structures* 13, 897–915.
- Kenane, E., Bakhti, H., Bentoumi, M., Djahli, F., 2021. A Dynamic Invasive Weeds Optimization Applied to Null Control of Linear Antenna Arrays with Constrained DRR. *Advanced Electromagnetics* 10, 52–61.
- Kennedy, J., Eberhart, R., 1995. Particle swarm optimization, in: *Proceedings of ICNN'95 - International Conference on Neural Networks*. Presented at the Proceedings of ICNN'95 - International Conference on Neural Networks, pp. 1942–1948 vol.4. <https://doi.org/10.1109/ICNN.1995.488968>
- Khatir, S., Tiachacht, S., Thanh, C.-L., Tran-Ngoc, H., Mirjalili, S., Abdel Wahab, M., 2022. A robust FRF damage indicator combined with optimization techniques for damage assessment in complex truss structures. *Case Studies in Construction Materials* 17, e01197. <https://doi.org/10.1016/j.cscm.2022.e01197>
- L. Ho Viet, T. Trinh Thi, and B. Ho Xuan, “Swarm intelligence-based technique to enhance performance of ANN in structural damage detection,” *Transport and Communications Science Journal*. vol. 73, no. 1, pp. 1–15, Jan. 2022, doi: 10.47869/tcsj.73.1.1.
- Mirjalili, S., 2015. Moth-flame optimization algorithm: A novel nature-inspired heuristic paradigm. *Knowledge-based systems* 89, 228–249.
- Mirjalili, S., Gandomi, A.H., Mirjalili, S.Z., Saremi, S., Faris, H., Mirjalili, S.M., 2017. Salp Swarm Algorithm: A bio-inspired optimizer for engineering design problems. *Advances in engineering software* 114, 163–191.
- Mirjalili, S., Mirjalili, S.M., Lewis, A., 2014. Grey wolf optimizer. *Advances in engineering software* 69, 46–61.
- Mostafa, M., Tawfik, M., 2016. Crack detection using mixed axial and bending natural frequencies in metallic Euler-Bernoulli beam. *Latin American Journal of Solids and Structures* 13, 1641–1657.
- Nguyen, T.C.N., Dang, T.H., Nguyen, H.Q., Tran, N.H., 2021. Experimental study of ground vibration caused by construction activities of metro line 1 project in Ho Chi Minh city. *Science Journal of Transportation* 68–78.
- Ngoc Long Nguyen, Huu Q.N., Ngoc Lan Nguyen, Tran H.N., 2023. Performance evaluation of the artificial hummingbird algorithm in the problem of structural damage identification. *Transport and Communications Science Journal* 74, 413–427. <https://doi.org/10.47869/tcsj.74.4.3>

Nguyen-Ngoc, L., Do, T.A., Hoang, V.H., Hoang, T.T., Tran, T.D., 2023. Equivalent Convective Heat Transfer Coefficient for Boundary Conditions in Temperature Prediction of Early-Age Concrete Elements Using FD and PSO. *KSCE Journal of Civil Engineering* 1–13.

Shahriari, B., Ravari, M.R., Yousefi, S., Tajdari, M., 2016. A heuristic algorithm based on line-up competition and generalized pattern search for solving integer and mixed integer non-linear optimization problems. *Latin American Journal of Solids and Structures* 13, 224–242.

Tran-Ngoc, N., Khatir, S., De Roeck, G., Nguyen, L., Bui, T.T., Abdel Wahab, M., 2020a. An efficient approach for model updating of a large-scale cable-stayed bridge using ambient vibration measurements combined with a hybrid metaheuristic search algorithm. *Smart Structures and Systems* 25, 487–499.

Tran-Ngoc, H., He, L., Reynders, E., Khatir, S., Le-Xuan, T., De Roeck, G., Bui-Tien, T., Wahab, M.A., 2020b. An efficient approach to model updating for a multispan railway bridge using orthogonal diagonalization combined with improved particle swarm optimization. *Journal of Sound and Vibration* 476, 115315.

Tran-Ngoc, H., Khatir, S., De Roeck, G., Bui-Tien, T., Nguyen-Ngoc, L., Abdel Wahab, M., 2018. Model updating for Nam O bridge using particle swarm optimization algorithm and genetic algorithm. *Sensors* 18, 4131.

Tran-Ngoc, H., Le-Xuan, T., Khatir, S., De Roeck, G., Bui-Tien, T., Abdel Wahab, M., 2023. A promising approach using Fibonacci sequence-based optimization algorithms and advanced computing. *Scientific Reports* 13, 3405.

Yang, X.-S., Deb, S., 2014. Cuckoo search: recent advances and applications. *Neural Computing and applications* 24, 169–174.

YiFei, L., MaoSen, C., H. Tran-Ngoc, Khatir, S., Abdel Wahab, M., 2023. Multi-parameter identification of concrete dam using polynomial chaos expansion and slime mould algorithm. *Computers & Structures* 281, 107018. <https://doi.org/10.1016/j.compstruc.2023.107018>.